

Supplementary information:

Collagen-based breathable, humid-ultrastable and degradable on-skin device

Le Ke,¹ Yaping Wang,¹ Xiaoxia Ye,¹ Wei Luo,² Xin Huang,^{*2} and Bi Shi²

¹*Department of Biomass Chemistry and Leather Engineering, Sichuan University, Chengdu
610065, P.R. China*

²*National Engineering Laboratory for Clean Technology of Leather Manufacture, Sichuan
University, Chengdu 610065, P.R. China*

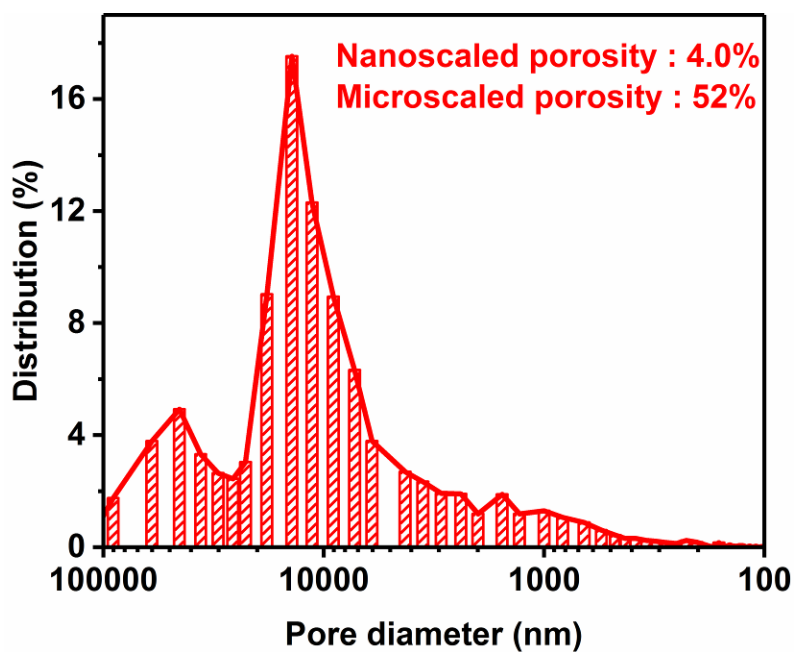


Fig. S1. Pore size distribution of cow skin with grain surface removed, which has with the nanoscaled porosity of 4.0% and microscaled porosity of 52%.

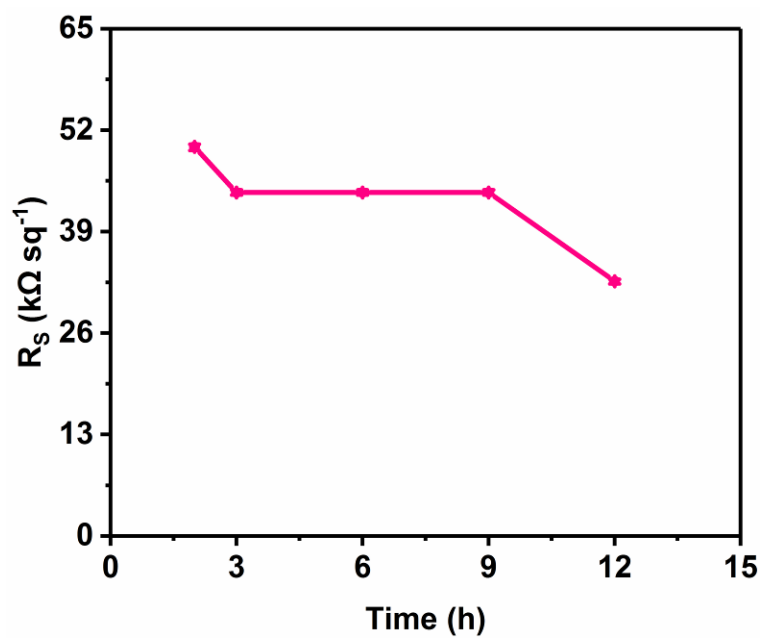


Fig. S2. The surface resistance (R_s) of cowskin after the *in situ* growth of polypyrrole for different growth times.

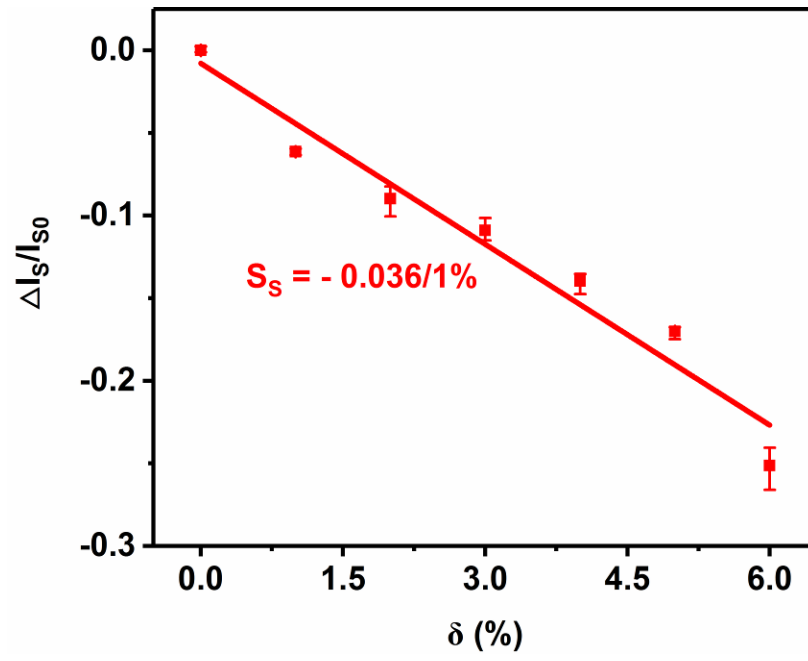


Fig. S3. The stretching sensitivity of the sensory skin.

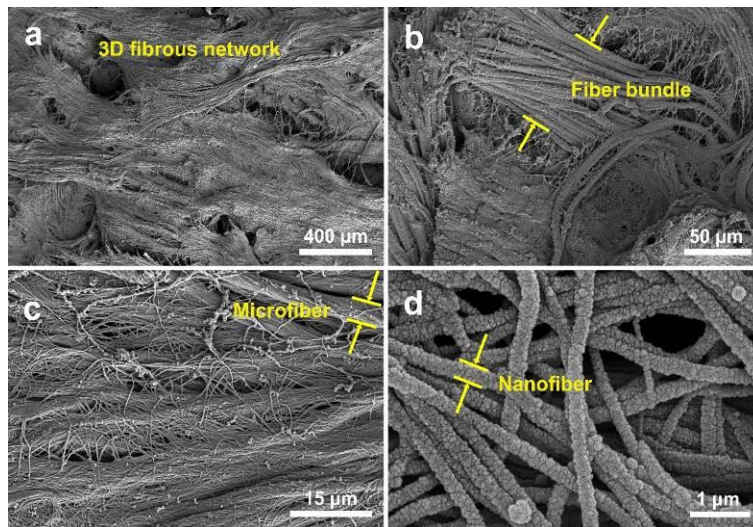


Fig. S4. The SEM images of sensory skin showing the hierarchically fibrous structure from fibrous network (a) to fiber bundle (b) and microfiber (c) and nanofiber (d).

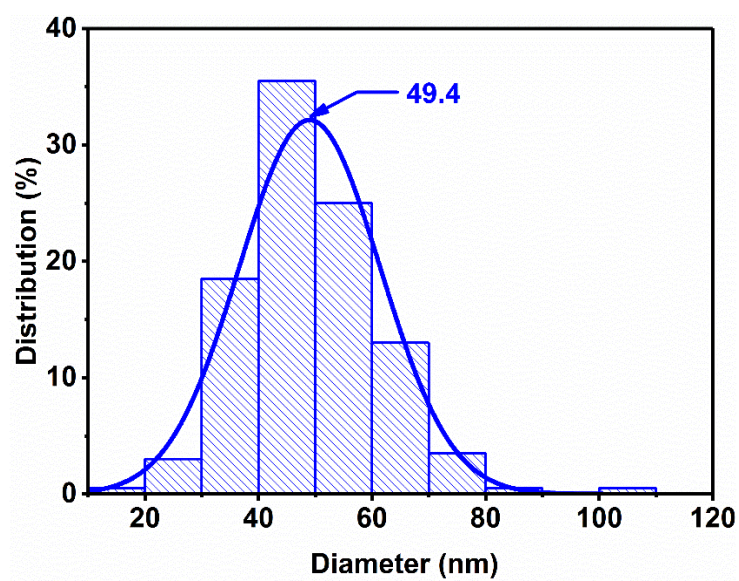


Fig. S5. The particle size distribution of polypyrrole NPs that were *in situ* grown onto the hierarchical fiber scaffold of cowskin.

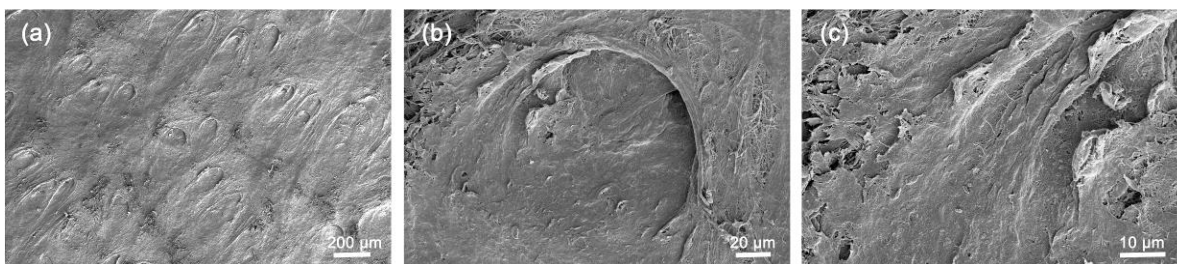


Fig. S6. The SEM images showing the grain surface of the cowskin (a-c).

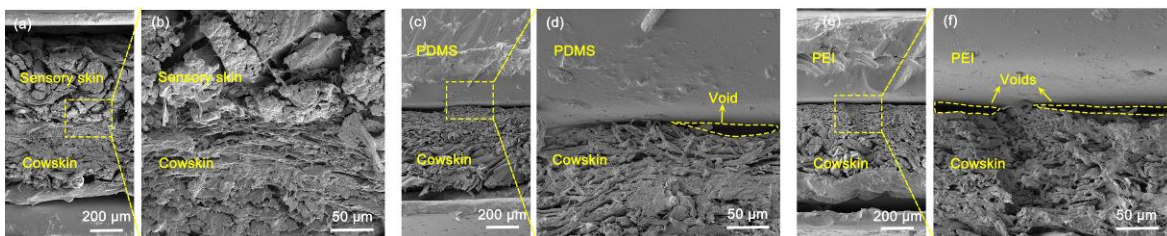


Fig. S7. The SEM images showing the cross-sections of closely packed sensory skin-cowskin (a, b), PDMS-cowskin (c, d) and PEI-cowskin (e, f).



Fig. S8. Digital photo of sensory skin device comprised of two sensory skins (60 mm × 25 mm) placed face-to-face.

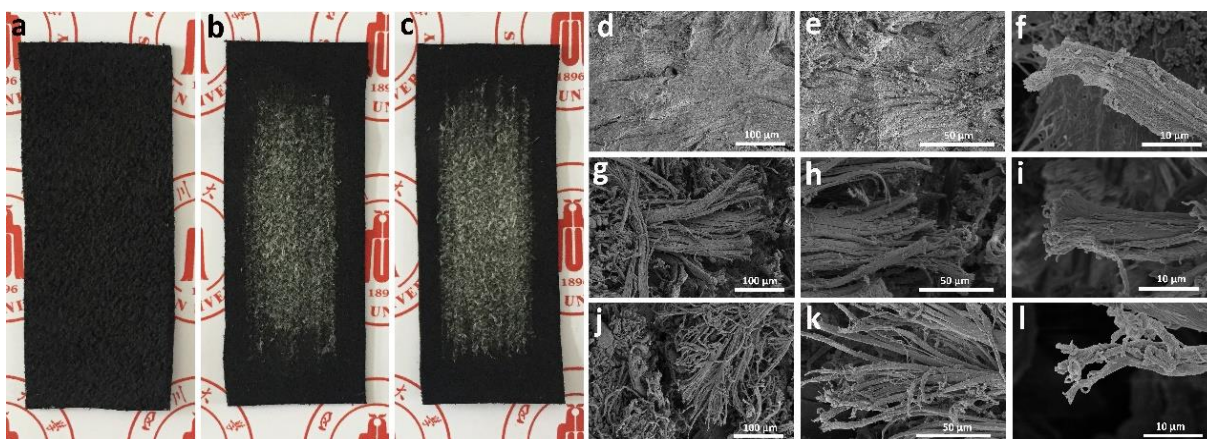


Fig. S9. Digital photos of sensory skin without (a) and with 20 (b) and 50 (c) cycles of sandpaper abrasion, and the corresponding SEM images of sensory skin without (d-f) and with 20 (g-i) and 50 (j-l) cycles of sandpaper abrasion.

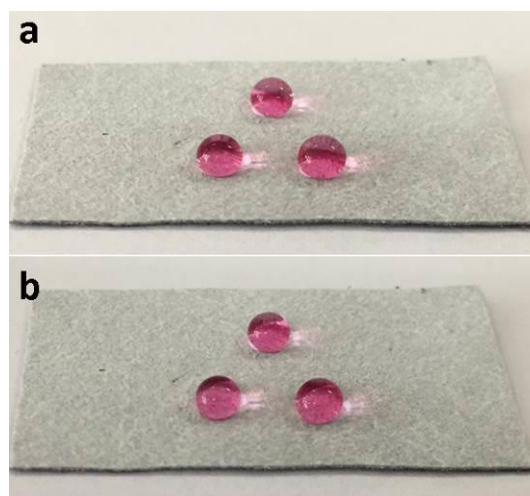


Fig. S10. Digital photos showing the temporary hydrophobicity of cow skin by dropping water droplets on the surface of cow skin after 0 min (a), and 2 min (b).

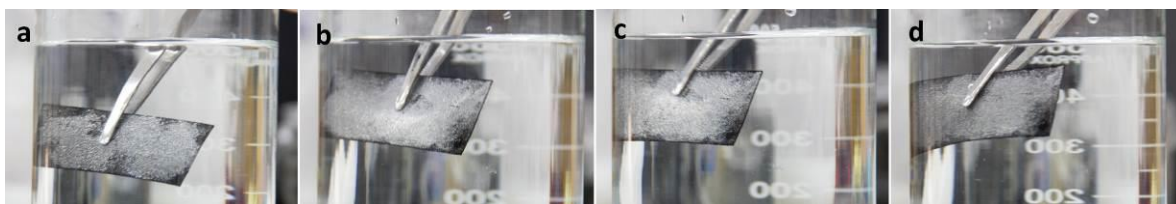


Fig. S11. Digital photos showing the silver mirror-like appearance by immersing superhydrophobic sensory skin in aqueous solution for the 5th (a), 10th (b), 15th (c) and 20th (d) time.

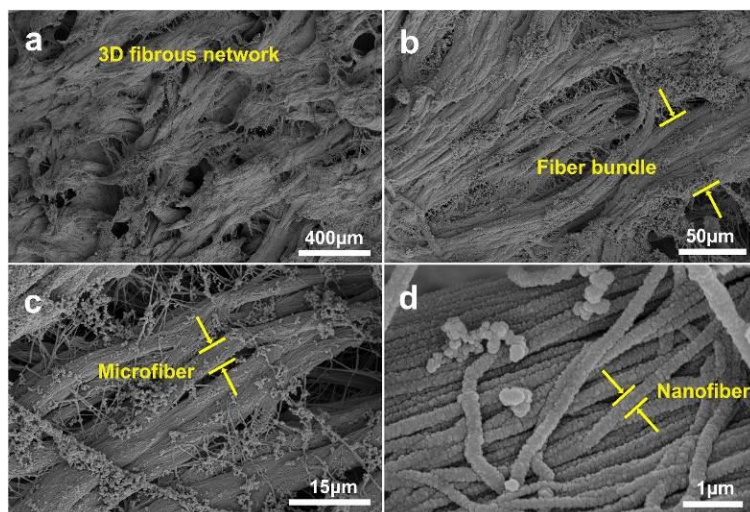


Fig. S12. SEM images of superhydrophobic sensory skin showing the well retained hierarchically fibrous structure.

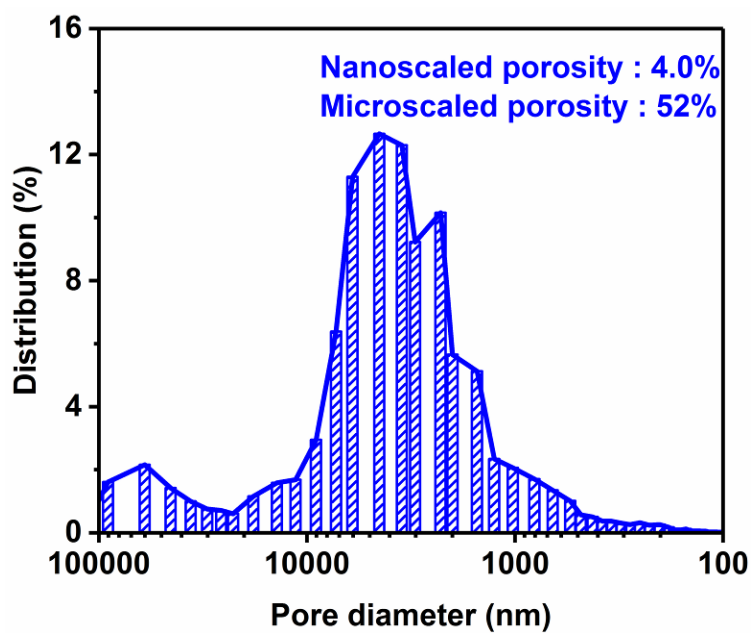


Fig. S13. Pore size distribution of superhydrophobic sensory skin with the nanoscaled porosity of 4.0% and microscaled porosity of 52%.

Table S1. Comparison of sensitivity between sensory skin and other pressure sensitive e-skins.

Sample	Sensitivity	Substrate	Reference
Pressure sensor based on nanowires/graphene	$9.4 \times 10^{-3} \text{ kPa}^{-1}$	PI	[1]
Graphene field-effect transistors-based pressure sensor	0.12 kPa^{-1}	Graphene field-effect transistors	[2]
Hydrogel-based pressure sensor	0.05 kPa^{-1}	PAM-PVA	[3]
Pressure sensor based on cotton thread	0.0156 kPa^{-1}	Cotton thread	[4]
Sensory skin	0.144 kPa^{-1}	Cowskin	This work

Table S2. Comparison of detection limit between sensory skin and previously reported pressure sensitive e-skins.

Sample	Detection limit	Substrate	Reference
PDMS-based electronic skin	0.6 Pa	PDMS	[5]
Rubber-based pressure sensor	3 Pa	PDMS	[6]
Nanofibres-based strain-gauge sensor	5 Pa	PDMS	[7]
PDMS-based pressure sensor	13 Pa	PDMS	[8]
Sensory skin	0.188 Pa	Cowskin	This work

REFERENCES

- 1 Z. Chen, Z. Wang, X. Li, Y. Lin, N. Luo, M. Long, N. Zhao and J. B. Xu, *ACS Nano*, 2017, **11**, 4507–4513.
- 2 Q. Sun, D. H. Kim, S. S. Park, N. Y. Lee, Y. Zhang, J. H. Lee, K. Cho and J. H. Cho, *Adv. Mater.*, 2014, **26**, 4735–4740.
- 3 G. Ge, Y. Zhang, J. Shao, W. Wang, W. Si, W. Huang and X. Dong, *Adv. Funct. Mater.*, 2018, **28**, 1802576.
- 4 Y. Tai and G. Lubineau, *Adv. Funct. Mater.*, 2016, **26**, 4078–4084.
- 5 X. Wang, Y. Gu, Z. Xiong, Z. Cui and T. Zhang, *Adv. Mater.*, 2014, **26**, 1336–1342.
- 6 S. C. B. Mannsfeld, B. C. K. Tee, R. M. Stoltenberg, C. V. H. H. Chen, S. Barman, B. V. O. Muir, A. N. Sokolov, C. Reese and Z. Bao, *Nat. Mater.*, 2010, **9**, 859–864.
- 7 C. Pang, G. Y. Lee, T. Kim, S. M. Kim, H. N. Kim, S. H. Ahn and K. Y. Suh, *Nat. Mater.*, 2012, **11**, 795–801.
- 8 S. Gong, W. Schwalb, Y. Wang, Y. Chen, Y. Tang, J. Si, B. Shirinzadeh and W. Cheng, *Nat. Commun.*, 2014, **5**, 3132.

Supplementary Movie Captions

Movie S1. Real-time detection of wrist pulse by sensory skin device.

Movie S2. Real-time detection of jugular venous pulses by the sensory skin device.

Movie S3. Real-time detection of apexcardiogram by the sensory skin device.

Movie S4. Real-time detection of throat muscle movement when speaking the word “OK”.

Movie S5. Real-time detection of throat muscle movement when speaking the word “sensor”.

Movie S6. Real-time detection of throat muscle movement when speaking the word “leather”.

Movie S7. Real-time detection performance of the sensory skin device by dropping water on the surface of superhydrophobic sensory skin.

Movie S8. Real-time detection performance of the sensory skin device by pouring water on the surface of superhydrophobic sensory skin.

Movie S9. Demonstration of 10 repetitive bending cycles of the sensory skin.